Journal of The Electrochemical Society, **154** (9) H778-H781 (2007)
0013-4651/2007/154(9)/H778/4/$20.00 © The Electrochemical Society

Silicon Epitaxial Growth on Poly-Si Film by HWCVD for Low-Temperature Poly-Si TFTs

Seung Ryul Lee, Kyung Min Ahn, and Byung Tae Ahn*,z

Department of Materials Science and Engineering, Korea Advanced Institute of Science and Technology, 373-1 Guseong-dong, Yuseong-gu, Daejeon 305-701, South Korea

A two-step process consisting of the preparation of poly-Si seed film by vapor-induced crystallization and the growth of an epitaxial Si layer on the poly-Si seed film via hot-wire chemical vapor deposition (HWCVD) is introduced to obtain a high-quality poly-Si film at a temperature below 500°C. The epitaxial Si by HWCVD was successfully grown on the poly-Si seed film at 450°C, and the crystallinity of the poly-Si seed film was maintained up to the surface of the epitaxial Si. With the two-step process, it was observed that the grain size was enlarged twofold compared to that of the poly-Si seed film. It was also found that the grain-boundary defect density was reduced. Moreover, the concentration of Ni and Al, which were introduced for the crystallization of a-Si, was lower at the surface.
 [DOI: 10.1149/1.2752030]

Manuscript submitted April 2, 2007; revised manuscript received May 1, 2007. Available electronically July 10, 2007.

There has been increasing interest in low-temperature polycrystalline silicon (poly-Si) films for thin-film transistors (TFTs), which are used in display electronics such as active matrix liquid crystal displays (AMLCDs) and active matrix organic light-emitting displays (AMOLEDs).[1,2] Poly-Si thin films are traditionally fabricated by the solid-phase crystallization (SPC) of amorphous Si (a-Si) thin films due to larger grains and better crystal quality compared to those of directly deposited poly-Si thin films. Unfortunately, the SPC process requires tens of hours to crystallize a-Si films even at 600°C, which is too high a temperature for large-area glass substrates.[3,4] Therefore, many methods such as metal-induced crystallization (MIC),[5,6] metal-induced lateral crystallization (MILC),[7,8] metal-induced crystallization through a cap (MICC),[9] and vapor-induced crystallization (VIC)[10] have been employed to enhance the crystallization of a-Si films. However, poly-Si films fabricated by these methods utilizing the reaction between metals and the a-Si film inherently contain a high density of metal impurities and grain-boundary defects, deteriorating the electrical properties of the low-temperature poly-Si TFTs.

Recently, hot-wire chemical vapor deposition (HWCVD) has been considered as a new method for low-temperature poly-Si and epitaxial Si films, as the catalytic or pyrolytic decomposition of precursor gases such as SiH_4 and H_2 occurs only on the surface of the heated wire. Moreover, HWCVD has many advantages, including a high deposition rate, low equipment cost, no fundamental limits to scale-up, and absence of ion bombardment (plasma-free process).[11-14]

In this paper, an approach is proposed for the fabrication of high-quality poly-Si films using a two-step process with a process temperature below 500°C. The first step involves the preparation of poly-Si seed films at 480°C by the VIC process, and the second step is the growth of an epitaxial Si layer at 450°C by HWCVD on the VIC poly-Si seed films. From this approach, it was found that the grain size of the poly-Si films was enlarged and that the defects at the grain boundary were reduced. Moreover, the levels of metal contaminations such as Al and Ni on the film surface were lowered.

Experimental

Figure 1 shows the schematics of the two-step process used to fabricate the high-quality poly-Si films in this study. a-Si films 100 nm thick, which were deposited on oxidized Si wafers, were crystallized by the VIC process using a vapor transport of Al/Ni chloride.[10] With this method, two separate heating zones (a source zone and an annealing zone) were required. The source was composed of $AlCl_3/NiCl_2$ = 10:1 and the temperature of the source zone was fixed at 200°C for source evaporation. The temperature of the annealing zone was maintained at 480 or 500°C for the crystallization of the a-films, and the Al/Ni chloride vapor was transported from the source zone to the annealing zone via an Ar flow with a flow rate of 0.5 L/min during the crystallization process.

After the crystallization of the a-Si film, the sample was cleaned in a H_2SO_4/H_2O_2 solution and dipped in a 2% HF solution in order

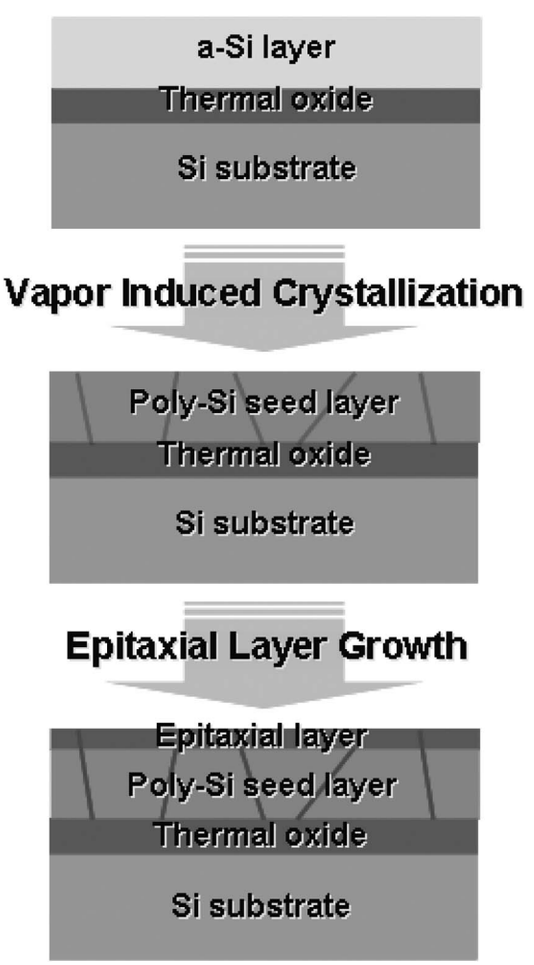

Figure 1. Schematics of the two-step process to fabricate the high-quality poly-Si films in this work.

* Electrochemical Society Active Member.
z E-mail: btahn@kaist.ac.kr

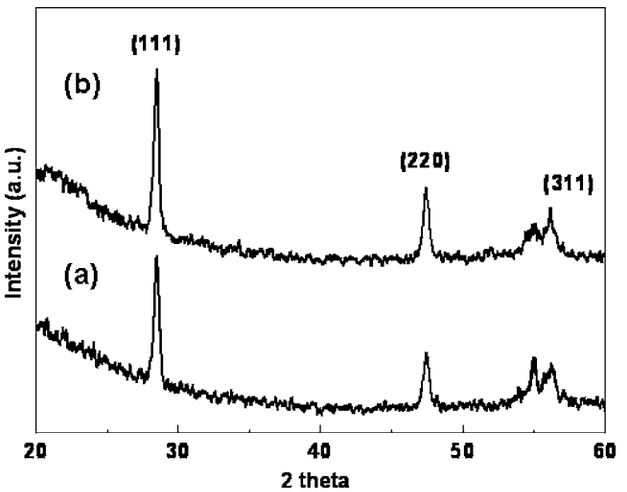

Figure 2. XRD patterns of (a) the poly-Si seed film produced using the VIC method and (b) the sample with an epitaxial layer on the VIC poly-Si seed film (epi-Si/poly-Si structure).

to remove metal residue and the surface oxide. Following this, it was immediately loaded into a HWCVD system. An epitaxial Si layer with a thickness of 40 nm was then grown on the poly-Si seed film by HWCVD at 450°C using 20% diluted SiH_4 in Ar, and its growth rate was 2.6 Å/s. In the HWCVD system, W-shaped tungsten wire of 0.5 mm diameter was positioned 4.5 cm away from the substrate and was heated to approximately 1900°C as measured by optical pyrometer. The base pressure was under 5×10^{-7} Torr and the working pressure was maintained at 100 mTorr during the growth of the epitaxial layer.

The surface morphology and uniformity of the poly-Si films were observed by optical microscopy (OM) and scanning electron microscopy (SEM). The crystal structure and crystallinity were determined by X-ray diffraction (XRD). A transmission electron microscope (TEM) was used to confirm the microstructure and lattice arrangement at the epitaxial Si/VIC poly-Si interface, and a secondary ion mass spectroscope (SIMS) was employed to investigate the distribution of metal impurities such as Al and Ni in the poly-Si films.

Results and Discussion

Figure 2 shows the XRD patterns of (a) a poly-Si seed film by the VIC method and (b) a sample with an epitaxial layer on the VIC poly-Si seed film (epi-Si/poly-Si structure). The crystallization of a-Si to poly-Si by the VIC method at 480°C for 10 h is confirmed because strong diffraction peaks of Si(111), (220), and (311) appear in Fig. 2a. From the sample with the epi-Si/poly-Si structure (Fig. 2b), the diffraction patterns of the poly-Si, including Si(111), (220), and (311), are also seen. It was found that the peak intensity of these patterns slightly increases compared to that of the VIC poly-Si seed film. It seems that this change in the peak intensity is due to the increase of the total crystalline film thickness by the growth of the epitaxial Si on the VIC poly-Si seed film.

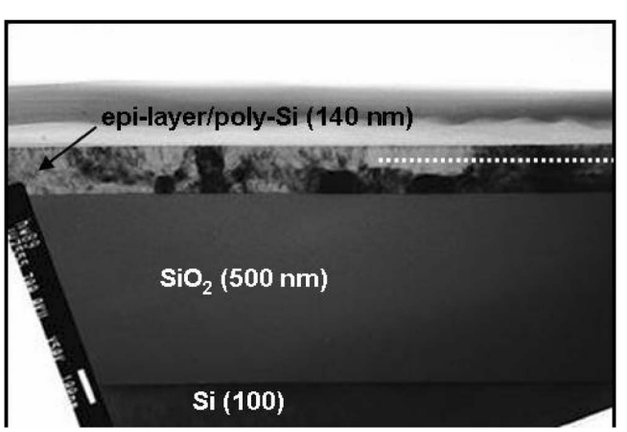

Figure 3. Cross-sectional TEM image of a sample with the epi-Si/poly-Si structure.

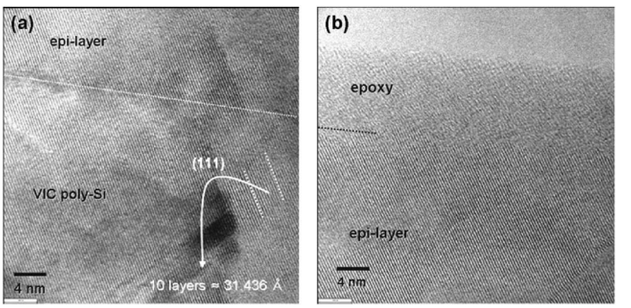

Figure 4. HRTEM images at (a) an epi-Si/poly-Si interface and (b) the surface of the epi-Si/poly-Si structure.

A cross-sectional TEM image of the sample with the epi-Si/poly-Si structure is shown in Fig. 3. The epi-Si/poly-Si interface is marked with a white line. There is no abrupt change in the contrast of the TEM image at the epi-Si/poly-Si interface, and it seems that the contrast of the TEM image in the epi-Si layer originated from the poly-Si seed film. The epi-Si/poly-Si interface is dimly visible in other magnified TEM analyses, but this is because contamination such as carbon or oxygen from a non-ultrahigh-vacuum (UHV) environment remains at the interface.

Figure 4 shows high-resolution TEM images (a) at the epi-Si/poly-Si interface and (b) on the surface of the epi-Si/poly-Si structure. The complete registry of the lattice can be seen across the epi-Si/poly-Si interface, indicating that the upper epi-Si layer is fully coherent with the poly-Si seed film. Additionally, it was found that the planar distance between each lattice in the poly-Si seed film (Fig. 4a) is identical to that near the surface of the epi-Si layer (Fig. 4b). This identity of the planar distance indicates that there is no epitaxy breakdown during the growth of the epitaxial Si and that the crystallinity of the poly-Si seed film is maintained up to the surface of the epitaxial Si.

Figure 5 shows the plan-view TEM images of (a) a poly-Si seed film and (b) a sample with the epi-Si/poly-Si structure. The poly-Si seed film was fabricated by the crystallization of a-Si film using the VIC method at 500°C for 8 h. From Fig. 5a, its grain size is estimated at approximately 4–5 μm, which is commonly smaller than

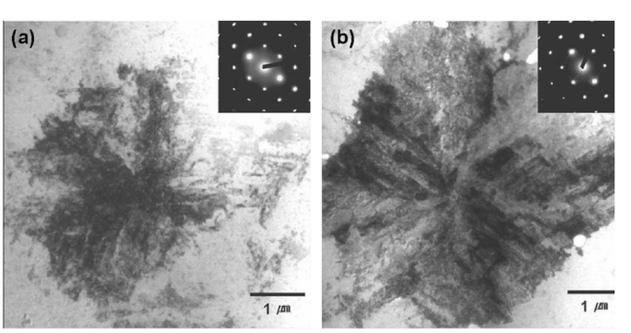

Figure 5. Plan-view TEM images of (a) the poly-Si seed film and (b) a sample with the epi-Si/poly-Si structure.

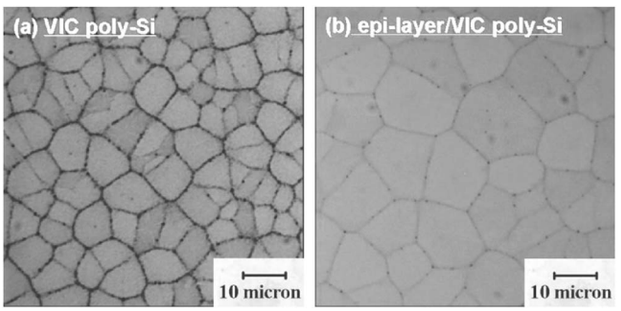

Figure 6. OM images of (a) the poly-Si seed film crystallized at 480°C and (b) a sample with epi-Si/poly-Si structure.

that of crystallized seed film at 480°C for 10 h. The spotlike selected area diffraction pattern (SADP) in the grain of the poly-Si seed film denotes that the grain has a quasi-monocrystalline phase. Moreover, the SADP in the grain of the epi-Si/poly-Si structure shown in Fig. 5b shows only a spotlike pattern, and there is no ring pattern caused by a microcrystalline phase or polycrystalline phase, indicating that the orientation of the underlying grain in the poly-Si seed film is consistent with that of the upper grain in the epi-Si layer. Therefore, it is confirmed that epitaxial Si can be successfully grown on a poly-Si seed film by HWCVD at 450°C.

In order to investigate the surface morphology and the microstructure over a large area, an OM analysis was performed. Figure 6 shows OM images of (a) a poly-Si seed film crystallized at 480°C and (b) a sample with epi-Si/poly-Si structure. Prior to the OM analysis, Secco etching (CrO_3/49% HF/H_2O = 0.75 M:1:100) was performed to see grain boundaries clearly and to remove metal impurities. From both OM images, it is observed that the grains are impinged together and display various polygonal disk shapes. A great difference exists, however, between the grain size of the poly-Si seed film and the sample with the epi-Si/poly-Si structure, with grain sizes of approximately 7 μm and about 15 μm, respectively. Namely, the grain size after the growth of the epitaxial Si on the poly-Si seed film is twice as large as that of the poly-Si seed film. It is guessed that the increase in the grain size is related to the mergence of adjacent grains with low angle boundary in the seed film or the preferential epitaxial growth of grains with a particular orientation. More detailed crystallographic and microstructural analyses are required. The increase in the grain size indicates a decrease of the grain boundary density with the crystalline imperfection and a decrease of the metal impurities of Ni and $NiSi_2$ at the grain boundary, which act as trapping sites to deteriorate the electrical properties of poly-Si TFTs. Therefore, this epi-Si/poly-Si structure has the advantage of reducing the density of grain boundaries and trapping sites, and it is considered that this two-step process can contribute to an improvement of the device performance.

In addition, it was observed that the grain boundary of the epitaxial Si is very narrow and sharp, while that of the poly-Si seed film is broad and rough, as shown in Fig. 6. After the Secco etching, the magnified microstructure at the grain boundary was analyzed by SEM. In Fig. 7a, it was observed that many etching holes at the grain boundary in the poly-Si seed film exist and that they are widely distributed. On the other hand, fewer etching holes at the grain boundary in the epitaxial Si were found, as shown in Fig. 7b, leading to the OM image with the sharp grain boundary shown in Fig. 6b. In particular, it was reported that an addition of Ni for the crystallization of a-Si causes the Ni to accumulate at the grain boundary, as the growth front of the growing grain consists of $NiSi_2$ and the grain boundary is formed when the growing fronts impinge together.[15,16] Therefore, it seems that these etching holes originate mainly from the etching of $NiSi_2$. Moreover, it is expected that the metal contamination at the surface of the poly-Si film can be reduced by using the epi-Si/poly-Si structure.

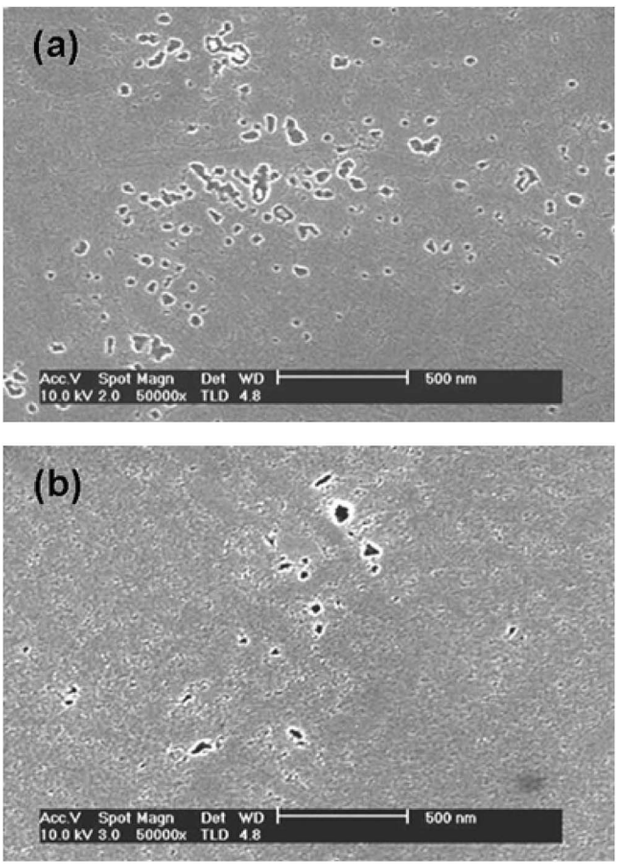

Figure 7. SEM images at the grain boundary of (a) the poly-Si seed film and (b) a sample with epi-Si/poly-Si structure.

Figure 8 shows SIMS profiles of Ni and Al in (a) a poly-Si seed film and (b) an epi-Si/poly-Si structure. In the poly-Si seed film, Ni is concentrated at the surface with a value of 3×10^{19} cm^{-3} and is uniformly distributed through the complete film thickness with a value of 10^{19} cm^{-3}. In addition, the Al concentration at the surface of the poly-Si seed film is 10^{19} cm^{-3} and sharply drops below 10^{16} cm^{-3} at a depth of nearly 25 nm. The distribution of Ni and Al in the epi-Si/poly-Si structure in Fig. 8b is very different from that in the poly-Si seed film. The Ni concentration in the epi-Si layer decreases gradually below 10^{19} cm^{-3} as the epitaxial layer grows, and falls to 2–3 $\times$ 10^{17} cm^{-3} at the surface. It seems that the decrease by one hundredth of a part in the Ni concentration occurs because the diffusivity of Ni is very low at an epitaxy temperature of 450°C and because the grain boundary density where Ni is accumulated is lower in the epi-Si/poly-Si structure, as shown in Fig. 6b and 7b. In the epi-Si/poly-Si structure, the Al concentration at the surface is reduced to 4×10^{18} cm^{-3}, which is half that at the surface in the poly-Si seed film, and that profile has a peak point at a depth of 40 nm (epi-Si/poly-Si interface). Consequently, it was found that the low-temperature epitaxial growth on the poly-Si seed film by using the HWCVD has the advantage of reducing metal contamination at the surface where TFTs are fabricated.

From the advantages of the two-step process presented in this study, it is expected that the growth of a thicker epitaxial Si layer on a thinner seed film might exhibit better overall film quality because the quality of epitaxial Si is superior to that of seed film. Further experimentation for the growth of thicker epitaxial Si on the thinner seed film will be continued in the future.

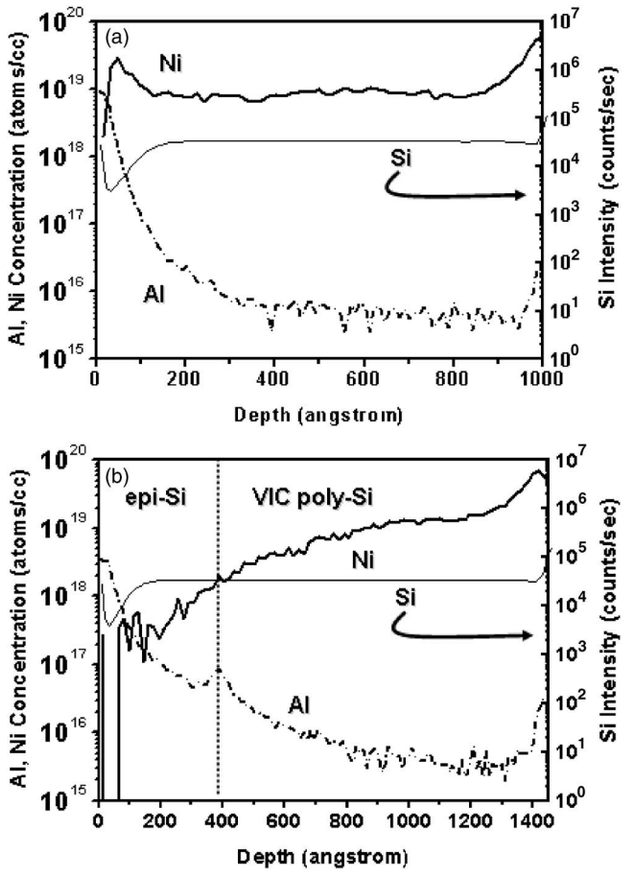

Figure 8. SIMS profiles of Ni and Al in (a) the poly-Si seed film and (b) the epi-Si/poly-Si structure.

Conclusions

To obtain a high-quality poly-Si film at a low temperature below 500°C, a two-step process was introduced. The first step involves the preparation of a poly-Si seed film at 480°C using the VIC process, and the second step involves the growth of an epitaxial Si layer at 450°C by HWCVD on the VIC poly-Si seed film. From planar and cross-sectional TEM analyses, it was confirmed that epitaxial Si by HWCVD at 450°C was successfully grown on the poly-Si seed film and that the crystallinity of the poly-Si seed film was maintained up to the surface of the epitaxial Si. After the growth of the epitaxial Si on the poly-Si seed film, it was observed that the grain size was enlarged to twice that of the poly-Si seed film and the crystalline imperfection at the grain boundaries was reduced. In addition, it was found that this two-step process has the advantage of reducing the concentration of Ni and Al at the surface of the poly-Si where TFTs are fabricated.

Korea Advanced Institute of Science and Technology assisted in meeting the publication costs of this article.

References

1. M. Yuki and K. Kunigita, *IEEE Trans. Electron Devices*, **36**, 1934 (1989).
2. M. Stewart, R. S. Howell, L. Pires, and M. K. Hatalis, *IEEE Trans. Electron Devices*, **48**, 845 (2001).
3. E. Korin, R. Reif, and B. Mikic, *Thin Solid Films*, **167**, 101 (1988).
4. H. Zhang, N. Kusumoto, T. Imushima, and S. Yamazaki, *IEEE Electron Device Lett.*, **13**, 297 (1992).
5. O. Nast and S. R. Wenham, *J. Appl. Phys.*, **88**, 124 (2000).
6. C. Hayzelden, J. L. Batstone, and R. C. Cammarata, *Appl. Phys. Lett.*, **60**, 225 (1992).
7. S. W. Lee and S. K. Joo, *IEEE Electron Device Lett.*, **17**, 160 (1996).
8. J. H. Ahn and B. T. Ahn, *J. Electrochem. Soc.*, **148**, H115 (2001).
9. J. H. Choi, D. Y. Kim, B. K. Choo, W. S. Sohn, and J. Jang, *Electrochem. Solid-State Lett.*, **6**, G16 (2003).
10. J. H. Eom, K. U. Lee, and B. T. Ahn, *Electrochem. Solid-State Lett.*, **8**, G65 (2005).
11. H. Matsumura, *Jpn. J. Appl. Phys., Part 1*, **37**, 3175 (1998).
12. J. Thiesen, E. Iwaniczko, K. M. Jones, A. Mahan, and R. Crandall, *Appl. Phys. Lett.*, **75**, 992 (1999).
13. R. E. I. Schropp, *Thin Solid Films* **403–404**, 17 (2002).
14. H. Matsumura, A. Masuda, and H. Umemoto, *Thin Solid Films*, **501**, 58 (2006).
15. V. Subramanian and K. C. Saraswat, *IEEE Trans. Electron Devices*, **45**, 1934 (1998).
16. P. J. van der Zaag, M. A. Verheijen, S. Y. Yoon, and N. D. Young, *Appl. Phys. Lett.*, **81**, 3404 (2002).